

# ECGI Periodicity Unraveled: A Deep Learning Approach for the Visualization of Periodic Spatiotemporal Patterns in Atrial Fibrillation Patients

Alexander Lacki<sup>1</sup>, Ismael Hernández-Romero<sup>1</sup>, Maria S Guillem<sup>1</sup>, Andreu M Climent<sup>1</sup>

<sup>1</sup>ITACA Institute, Universitat Politècnica de València, Valencia, Spain

## Abstract

*This work proposes a novel deep learning based method for the identification of periodic patterns in Electrocardiographic Imaging (ECGI) signals and demonstrates its ability to identify, quantify, and visualize recurring patterns.*

*ECGIs from AF patients obtained prior to pulmonary vein isolation (PVI) are encoded to a lower-dimensional feature space using a 3D-CNN autoencoder, and further processed with principal component analysis to aggregate recurring patterns and quantify their contribution to the overall spatiotemporal propagation pattern.*

*Several markers are evaluated as potential predictors of AF recurrence. The variance captured by the first 3 principal components (PCs) varied from 19.8% to 59.2% ( $32.2 \pm 9.35$ ) in different patients showed an inter-segment correlation exceeding 64%. Similarly, the number of PCs necessary to explain 90% of variance in ECGI recordings varied from 20 to 90 ( $56.2 \pm 20.1$ ) demonstrating a varying number of propagation patterns across patients, which was reproducible intra-patient with an inter-segment correlation higher than 69%.*

*In addition, backpropagation-based saliency maps are computed to identify in which atrial regions the captured patterns occur. Saliency maps are visualized on 3D atrial models to aid in the interpretation and anatomical contextualization.*

## 1. Introduction

AF is characterized by an irregular electrical activity, and the quantification its regularity remains a challenging task. Previous works have evaluated regularity in electrophysiological signals, investigating spatiotemporal stability and variability. In [1] the authors demonstrated that spatiotemporal variability in 12-lead ECGs is a predictor of AF recurrence after catheter ablation. In another recent study [2] the authors demonstrated that electrophysiological spatiotemporal stability varies among different regions of the left atrial endocardium. Similarly, the authors in [3] have shown that periodic activation patterns in the epicardium are associated with re-entrant AF drivers, which, in turn, lead to spatiotemporally stable patterns on electrograms.

The previous findings may lead to the hypothesis that

ECGI could constitute a non-invasive method to identify regions with periodic behaviour, and that such regions could carry information regarding patient prognosis and the recurrence of AF after PVI. With this hypothesis in mind, this work presents a novel method for identifying and visualizing quasiperiodic AF patterns in ECGI maps, and illustrates its ability to identify, quantify, and localize periodic patterns.

## 2. Materials and Methods

### 2.1. Data Acquisition and Pre-Processing

Body surface potential recordings from 29 patients in AF were obtained prior to PVI. Atrial geometries were obtained from MRI imaging, while torso geometries were captured using a photogrammetry system. The acquisition and pre-processing protocols were previously described in detail in [4]. For each personalized atrial geometry, 2-dimensional conformal maps are computed to represent ECGI signals as sequences of square, 2-dimensional images using the method presented in [5]. Patients were followed-up 6-months after PVI and classified as recurrent or non-recurrent.

Videos of epicardial voltage in the atria are standardized such that each pixel is zero centred and has a standard deviation of 1. Values above 2.0 and below -2.0 are truncated, to prevent outliers.

### 2.2. Autoencoder Training and Encoding

Video segments are encoded to a lower-dimensional feature space using a 3D-CNN autoencoder, for which the architecture and training hyperparameters are determined empirically. Figure 1 shows a symbolic representation of a 3D-CNN autoencoder. The autoencoder is trained using the Adam optimizer [6] minimizing the mean squared error between input and output video segments. Once the appropriate autoencoder architecture is determined, video segments of the patients in our cohort are encoded to a lower dimensional space using only the encoder (Figure 1, purple). To capture the dynamic properties of the signal, video segments of 128ms with a step size of 8ms are employed, resulting in segments consisting of 16 images.

The generated encodings (Figure 1, yellow) are flattened into 1D vectors and processed using principal

component analysis resulting in a further dimensionality reduction and PCs that represent linear combinations of co-occurring spatiotemporal features in the encoding, captured by single variables.

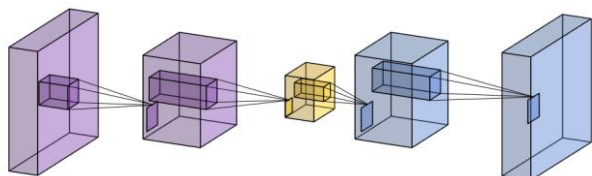


Figure 1. Schematic of a 3D-CNN autoencoder. Purple: Encoder which reduces the dimensionality of the input data to a latent space (yellow). Blue: Decoder which reconstructs the input video from the compressed information in the latent space.

### 2.3. Encoding Analysis

The encodings are analysed in terms of the variance captured by the first 3 PCs and the number of PCs necessary to capture 90% of the encoding variance. Differences in distributions across the two patient groups, recurrent and non-recurrent at 6-month follow-up, are assessed using the Mann-Whitney U test.

### 2.4. Visualization

To determine the localization of patterns captured by PCs, backpropagation-based saliency maps according to [7] are derived. By computing the derivative of each image within the input video to the encoder, with respect to the PC, heatmaps indicating pixel importance, hence the contribution of each pixel to the PCs are generated.

While natively the 3D-CNN autoencoder operates on a sequence of 2D images, saliency maps are reconstructed on the original 3-dimensional atrial geometries for easier visualization and interpretation. Saliency maps are compared to the phase of ECGI signals to investigate what propagation patterns are captured by the proposed method.

## 3. Results

### 3.1. Autoencoder Training and Encoding

The resulting autoencoder architecture is presented in table 1. The obtained configuration yields a mean squared error between input and reconstructed segments of 0.017 and 0.025 on the training and validation set respectively, which is deemed sufficient for the application.

Table 1. Autoencoder Architecture. Conv3D: 3D Convolution. L-ReLU: Leaky Rectified Linear Unit. Tanh: Hyperbolic Tangent.

| Layer No. | Layer Type  | Output Shape      | Activation Function |
|-----------|-------------|-------------------|---------------------|
| 0         | Input       | (16, 64, 64, 1)   | -                   |
| 1         | Conv3D      | (16, 64, 64, 128) | L-ReLU              |
| 2         | Max Pooling | (8, 32, 32, 128)  | -                   |
| 3         | Conv3D      | (8, 32, 32, 64)   | L-ReLU              |
| 4         | Max Pooling | (4, 16, 16, 64)   | -                   |
| 5         | Conv3D      | (4, 16, 16, 8)    | Tanh                |
| 6         | Max Pooling | (4, 8, 8, 8)      | -                   |
| 7         | Up-sampling | (4, 16, 16, 8)    | -                   |
| 8         | Conv3D      | (4, 16, 16, 64)   | L-ReLU              |
| 9         | Up-sampling | (8, 32, 32, 64)   | -                   |
| 10        | Conv3D      | (8, 32, 32, 128)  | L-ReLU              |
| 11        | Up-sampling | (16, 64, 64, 128) | -                   |
| 12        | Conv3D      | (16, 64, 64, 1)   | Linear              |

### 3.2. Encoding Analysis

Figure 2 portrays the phase computed on personal atrial geometries for the two patients with the lowest and highest number of PCs required to capture 90% variance (14 vs. 85, variance captured by the first 3 PCs: 53.2% vs. 30.2%). Notice that the patient in which less variance is captured by the first 3 PCs and requiring more PCs to capture 90% of variance displays a more complex activity with a higher number of simultaneous wavefronts.

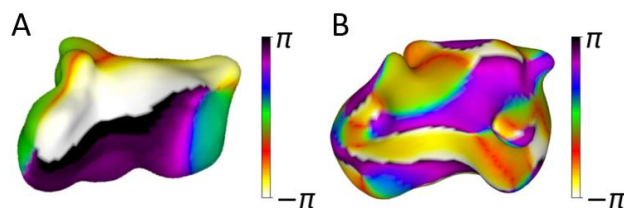


Figure 2. A: Phase computed on the atrial geometries of patients with simple (A) and complex atrial activity (B).

Joint plots of inter-segment correlations, and histograms of the evaluated parameters for the entire cohort are presented in Figure 3. The variance captured by the first three PCs varied from 19.8% to 59.2% ( $32.2 \pm 9.35$ ). The number of PCs necessary to explain 90% of variance in the encoding varied from 14 to 85 ( $53.6 \pm 19.7$ ) demonstrating varying degrees of spatiotemporal organization. These parameters were found to be reproducible intra-patient in different signal segments with correlations of 64%, and 69% respectively.

The Mann Whitney U test for the extracted parameters did not show significant differences between patients exhibiting AF recurrence at follow-up. The captured variance by the first 3 PCs and the number of PCs required to capture 90% of variance showed p-values of 0.073 and 0.27 respectively.

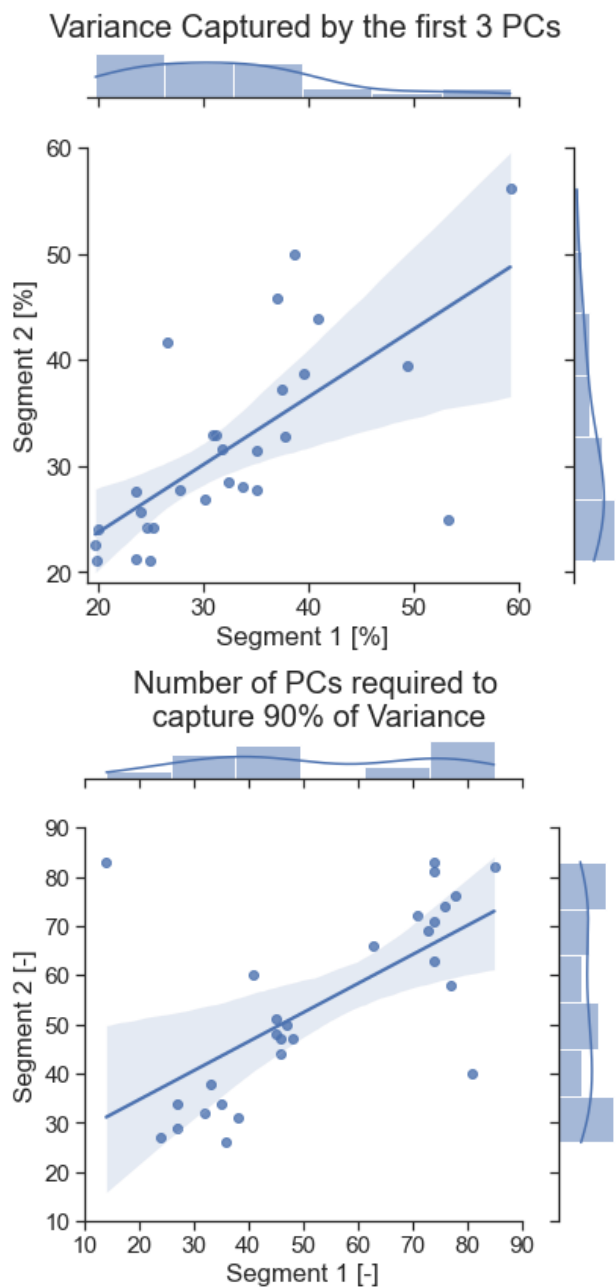


Figure 3. Correlation and histogram plots of extracted parameters for two separate segments in each patient. Top: Variance captured by the first 3 PCs. Bottom: Number of PCs required to capture 90% of variance.

### 3.3. Visualization

Two of the generated saliency maps are shown in Figure 4. Figure 4A shows the phase computed on the patient's geometry with a large propagation occurring in the atrial roof, and a rotor in the inferior pulmonary vein. It can be observed that that low-frequency, high variance PCs (Fig. 4B) capture conduction patterns spanning large regions of the atria, while the high-frequency, lower variance PCs (Fig. 4C) point towards the rotor in the pulmonary vein.

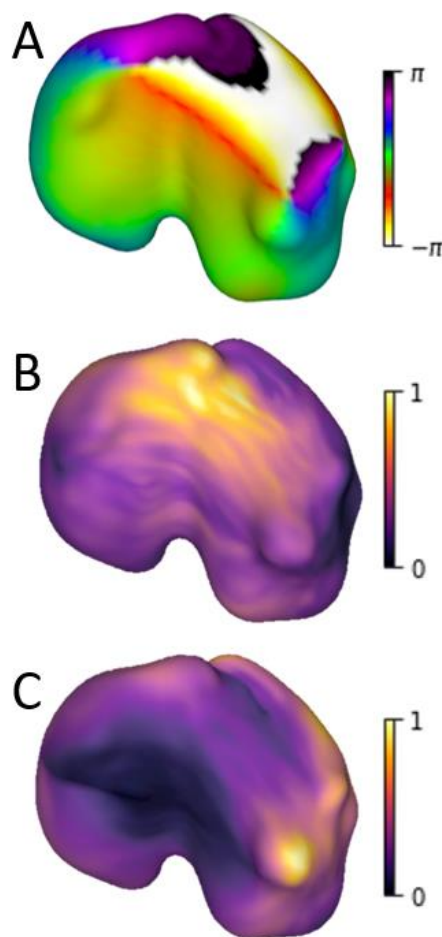


Figure 4. A: Phase of atrial activity on the patient's personalized geometry. B, C: Saliency computed for PCs with dominant frequencies of 5.65 and 16.1 Hz respectively.

## 4. Discussion

This work presents the first application of deep learning to the identification of periodic propagation patterns in ECGI recordings obtained from AF patients. It demonstrates that the varying degrees of complexity encountered in ECGI signals of AF patients can be quantified and visualized.

The presented method extends the previously mentioned works that have demonstrated different degrees of organization in electrophysiological recordings during AF. Unlike previous works, which evaluated the entire signal [1] or regions of the atria individually [2], this method inherently aggregates co-occurring patterns, and characterizes them based on their contribution to the whole atrial activity. Furthermore, the use of saliency maps for visualization demonstrates the ability to visualize the location of captured patterns on personalized patient geometries.

This study was performed on a small cohort of patients, all undergoing PVI, which made the evaluation of clinical implications and recurrence prediction difficult. Patients were described in terms of PCA markers, as well as spectral properties, and atrial anatomy was not considered for prediction. While this work does not evaluate the captured patterns within the anatomical context, it presents a method which localizes the captured patterns and visualizes the location on the personalized geometry, which could enable the contextualization of captured periodic patterns and atrial regions, and possibly aid in the identification of ablation targets.

Further, the presented method could be extended to a semantic description of the captured patterns. Such analysis could identify which captured patterns carry information relevant to patient treatment and ensure that saliency maps are generated based on clinical significance.

## 5. Conclusions

A novel method to assess the spatiotemporal behaviour of activation patterns in ECGI is presented, that captures different degrees of complexity in AF patients and visualizes the electrophysiological patterns. The method detects temporally co-occurring features and identifies spectral parameters of said features. Furthermore, it allows for the visualization of the patterns on 3-dimensional personalized geometries, which facilitates a contextualization of captured propagation patterns with anatomical atrial regions.

## Acknowledgments

This work was supported by PersonalizeAF project. This project has received funding from the European Union's Horizon 2020 research and innovation programme under the Marie Skłodowska-Curie grant agreement No 860974." Dr. Andreu M Climent is funded by the Agencia Estatal de Investigación of Ministry of Science of Spain through the Ramon y Cajal Grant RYC2018-024346-I. This project was partially funded by the CDTI-Cervera EXP 00124790 / IDI-20200226.

This publication reflects only the authors' view, and the funding Agencies are not responsible for any use that maybe made of the information it contains. The authors hold equity in Corify Care SL.

## References

- [1] Hidalgo-Muñoz, Antonio R et. al. Spectral and spatiotemporal variability ECG parameters linked to catheter ablation outcome in persistent atrial fibrillation. *Computers in biology and medicine* 2017;88;126-131.
- [2] Mann I. et. al. RETRO-MAPPING: A new approach to activation mapping in persistent atrial fibrillation reveals evidence of spatiotemporal stability. *Circulation: Arrhythmia and Electrophysiology*. 2021;14:e009602.
- [3] Skanes, A. et al. Spatiotemporal periodicity during atrial fibrillation in the isolated sheep heart. *Circulation* 1998;12;1236-1248.
- [4] Rodrigo M. et al., Noninvasive assessment of complexity of atrial fibrillation: Correlation with contact mapping and impact of ablation. *Circ. Arrhythmia Electrophysiol*. 2020;236-246.
- [5] Meng, T. et al. TEMPO: Feature-endowed teichmüller extremal mappings of point clouds. *ArXiv* 2016: n. pag.
- [6] Kingma, Diederik P. and Jimmy Ba. Adam: A method for stochastic optimization. *CoRR* abs/1412.6980 (2015): n. pag.
- [7] Simonyan, K. et al. Deep inside convolutional networks: Visualising image classification models and saliency maps. *Workshop at International Conference on Learning Representations* 2014; n. pag.

Address for correspondence:

Alexander Lacki

ITACA. Edificio 8G acceso B. Universitat Politècnica de València. Camino de Vera s/n. 46022 Valencia, Spain.

alacki@upvnet.upv.es